THE JOURNAL OF BIOLOGICAL CHEMISTRY VOL. 284, NO. 35, pp. 23872–23884, August 28, 2009

Gln-222 in Transmembrane Domain 4 and Gln-526 in Transmembrane Domain 9 Are Critical for Substrate Recognition in the Yeast High Affinity Glutathione Transporter, Hgt1p*[S]

Received for publication, March 17, 2009, and in revised form, July 2, 2009 Published, JBC Papers in Press, July 9, 2009, DOI 10.1074/jbc.M109.029728

Jaspreet Kaur[1] **and Anand K. Bachhawat**[2]

From the Institute of Microbial Technology, Sector 39-A, Chandigarh 160 036, India

Hgt1p, a member of the oligopeptide transporter family, is a high affinity glutathione transporter from the yeast *Saccharomyces cerevisiae*. We have explored the role of polar or charged residues in the putative transmembrane domains of Hgt1p to obtain insights into the structural features of Hgt1p that govern its substrate specificity. A total of 22 charged and polar residues in the predicted transmembrane domains and other conserved regions were subjected to alanine mutagenesis. Functional characterization of these 22 mutants identified 11 mutants which exhibited significant loss in functional activity. All 11 mutants except T114A had protein expression levels comparable with wild type, and all except E744A were proficient in trafficking to the cell surface. Kinetic analyses revealed differential contributions toward the functional activity of Hgt1p by these residues and identified Asn-124 in transmembrane domain 1 (TMD1), Gln-222 in TMD4, Gln-526 in TMD9, and Glu-544, Arg-554, and Lys-562 in the intracellular loop region 537–568 containing the highly conserved proline-rich motif to be essential for the transport activity of the protein. Furthermore, mutants Q222A and Q526A exhibited a nearly 4- and 8-fold increase in the K_m for glutathione. Interestingly, although Gln-222 is widely conserved among other functionally characterized oligopeptide transporter family members including those having a different substrate specificity, Gln-526 is present only in Hgt1p and Pgt1, the only two known high affinity glutathione transporters. These results provide the first insights into the substrate recognition residues of a high affinity glutathione transporter and on residues/helices involved in substrate translocation in the structurally uncharacterized oligopeptide transporter family.

Hgt1p or ScOpt1p, a polytopic membrane protein, from the yeast *Saccharomyces cerevisiae*, was the first high affinity glutathione transporter to be identified in any system (1). Hgt1p belongs to a relatively novel family of transporters, the oligopeptide transporter (OPT)[3] family, that contains a large number of fungal, plant, and prokaryotic members (2). The functional characterizations of a few of the fungal and plants members have demonstrated their ability to transport oligopeptides, glutathione, and metal-secondary amino acid conjugates by harnessing the proton gradient across the plasma membrane (3–7). Furthermore, these studies have also highlighted the physiological significance of this family in assimilation/mobilization of oligopeptides as nutrients in fungi and plants and in maintenance of metal homeostasis in plants. However, the majority of the members are yet uncharacterized and need to be defined with respect to their substrate specificity and physiological role.

A complete lack of information on the structural features of the OPT family further limits our understanding of this large, uncharacterized family. Identification of residues or motifs critical for substrate recognition among the functionally characterized members would enable functional characterization of the new members within the family. This has prompted us to initiate a systematic study on the structure-function characterization of Hgt1p as a representative of the OPT family. Not only is Hgt1p the best characterized member of the OPT family in terms of its substrate specificity, being also able to transport some oligopeptides albeit with low affinity (1, 7, 8), its native host *S. cerevisiae* is a well established model system and easily amendable for mutagenesis-based structure-function studies. We have recently investigated the role of the 12 native cysteine residues in the structural stability and the transporter activity of the protein where 2 of the cysteines were found to be essential for functionality (9). However, no hints on the important motifs or conserved amino acids of Hgt1p (or any other member of the OPT family) that could be involved in substrate recognition have been obtained so far. In the current study we have focused on the polar and charged residues in the transmembrane domains of Hgt1p to explore their role in substrate recognition.

Glutathione, the substrate for Hgt1p, is a hydrophilic substrate. Prior studies on structural characterization of transporters of the other hydrophilic substrates using biochemical and genetic strategies, such as site-directed mutagenesis and random mutagenesis, have established the role of polar and

* This work was supported by grant-in-aid projects (to A. K. B.) from the Department of Biotechnology and Departments of Science and Technology, Government of India.
[S] The on-line version of this article (available at http://www.jbc.org) contains supplemental Table 1 and Fig. 1.
[1] Recipient of a research fellowship from the Council of Scientific and Industrial Research, Government of India.
[2] To whom correspondence should be addressed. Tel.: 91-172-2636681; Fax: 91-172-2690585 or 91-172-2690632; E-mail: anand@imtech.res.in.

[3] The abbreviations used are: OPT, oligopeptide transporter; HA, hemagglutinin; PT, peptide transport; TMD, transmembrane domain; MES, 4-morpholineethanesulfonic acid; ICL, intracellular loop; MRP, multidrug-associated resistance protein.

charged residues in the transmembrane domains of transporters in recognition, binding, and translocation of substrates (10–18). The availability of the crystal structures of a few transporter proteins have further enabled direct visualization of such interactions between the key residues in the transmembrane domains and the substrate molecule (19–22). In light of these studies we anticipated that few of the charged or polar residues in the predicted transmembrane domains of Hgt1p would be involved in substrate recognition and translocation across the membrane. Hence, a total of 22 polar or charged amino acids spanning the predicted transmembrane domains of Hgt1p were subjected to alanine scanning and functionally characterized. Detailed biochemical characterizations of these mutants revealed that Asn-124, Gln-222, Gln-526, Glu-544, Arg-554, and Lys-562 are key residues for the transport activity of Hgt1p. As replacement of Gln-222 in TMD4 and Gln-526 in TMD9 with alanine resulted in a significant decrease in the affinity of the transporter for glutathione, it suggested that the two residues might directly participate in glutathione recognition as a substrate. These observations provide the first insights into substrate binding residues in Hgt1p, a member of a novel and important transporter family (OPT family).

EXPERIMENTAL PROCEDURES

Chemicals and Reagents—All the chemicals used in this study were obtained from commercial sources and were of analytical grade. Media components, fine chemicals, and reagents were purchased from Sigma Aldrich, HiMedia (Mumbai, India), Merck, USB Corp., or Difco. Oligonucleotides were purchased from Biobasic Inc. (Markham, ON, Canada). Restriction enzymes, Vent DNA polymerase, and TaqDNA polymerase and other DNA-modifying enzymes were obtained from New England Biolabs, (Beverly, MA). A DNA sequencing kit (ABI PRISM 3130 XL with dye termination cycle sequencing ready reaction kit) was obtained from PerkinElmer Life Sciences. Gel extraction kits and plasmid miniprep columns were obtained from Qiagen (Valencia, CA) or Sigma. [^{35}S]GSH (specific activity 1000 Ci mmol^{-1}) was purchased from Bhabha Atomic Research Centre, Mumbai, India. Hemagglutinin (HA)-tag (6E2) mouse monoclonal antibody and horse anti-mouse horseradish peroxidase-linked antibody were bought from Cell Signaling (Danvers, MA). Alexa Fluor® 488-conjugated goat anti-mouse antibody was obtained from Molecular Probes (Eugene, OR). Hybond ECL (nitrocellulose) membrane and ECL plus Western blotting detection reagents were purchased from Amersham Biosciences.

Strains, Media, and Growth Conditions—The *Escherichia coli* strain DH5α was used as a cloning host. The *S. cerevisiae* strain (ABC 817) bearing an HGT1 disruption in BY4741background (MATa his3Δ1 leu2Δ0 met15Δ0 ura3Δ0 hgt1Δ::LEU2) is deficient in glutathione uptake ability and was used in the experimental studies (1). The yeast strain was regularly maintained on yeast extract, peptone, and dextrose medium and grown at 28–30 °C. The yeast transformants were selected and maintained on synthetic defined minimal medium containing yeast nitrogen base, ammonium sulfate dextrose supplemented with adenine, histidine, leucine, lysine, methionine, tryptophan, and uracil at 50 mg/liter as per requirement. Growth, handling of bacteria and yeast, and all the molecular techniques used in the study were according to standard protocols (23, 24).

Site-directed Mutagenesis and Plasmid Construction—The double-tagged *HGT1*, tagged with hexahistidine epitope at the N terminus and HA tag at the C terminus (9), was subcloned downstream of the TEF promoter at BamHI and EcoRI site of a modified p416TEF vector (p416M1-TEF) in which all the restrictions sites flanking the BamHI and EcoRI restriction sites have been removed by blunting and re-ligation.

The resulting plasmid pTEFM1-His-HGT1-HA was used as a template to introduce two silent mutations to generate the restriction sites-MscI (1366) and XbaI (1584) in the wild-type *HGT1* gene using the QuikChange® site-directed mutagenesis kit with respective mutagenic oligonucleotides pairs given in supplemental Table 1. This modification generated a recombinant *HGT1* gene that was unaltered in the encoded protein product but had additional restriction sites to facilitate cloning and screening of mutant DNA (Fig. 1). This modified gene product was used as a template for site-directed mutagenesis for creation of different site-directed mutants of Hgt1p using either the QuikChange® site-directed mutagenesis kit or the splice overlap extension strategy. The different mutagenic oligonucleotides pairs used for generation of these mutants are given in supplemental Table 1.

For using the QuikChange® site-directed mutagenesis kit to generate the mutants, the double-tagged *HGT1* (N-His-HGT1-HA) was subcloned into pBSK vector and used as a template together with different mutant primer pairs (supplemental Table 1) in mutagenic PCR set up as per the manufacturer's instructions. The resulting mutants were sequenced to confirm the presence of the desired nucleotides changes and rule out any undesired mutations introduced during the mutagenic procedure. The fragments containing the mutations were subcloned back into the TEF vector background (pTEFM1-His-HGT1^{m}-HA) using the appropriate restriction sites for subsequent analyses. While using the splice overlap extension strategy, the mutations were directly generated in the TEF vector background, and the resulting mutations were confirmed by sequencing the appropriate regions.

The Plate "Dual Complementation-cum-toxicity" Assay—The development of the assay and procedure has been described previously (9). Briefly, the yeast strain *met15Δhgt1Δ* (ABC 817) was transformed with a single copy, centromere vector expressing wild type, or different *HGT1* mutants expressed downstream of the TEF promoter. Transformants were grown in minimal media containing methionine and other supplements without uracil overnight. These cultures were reinoculated in the same media and allowed to grow till they reached exponential phase. Equal numbers of cells were harvested, washed with water, and resuspended in sterile water to an A_{600} of 0.2. These were serially diluted 1:10, 1:100, and 1:1000. 10 μl of these cell resuspensions were spotted on minimal medium containing different concentrations of glutathione (15, 30, 50, 100, 150, 200 μM) or methionine (200 μM) as the sole organic sulfur source. The plates were incubated at 30 °C for 2–3 days, and photographs were taken. Only the data obtained with 15, 50, and 200 μM GSH have been shown.

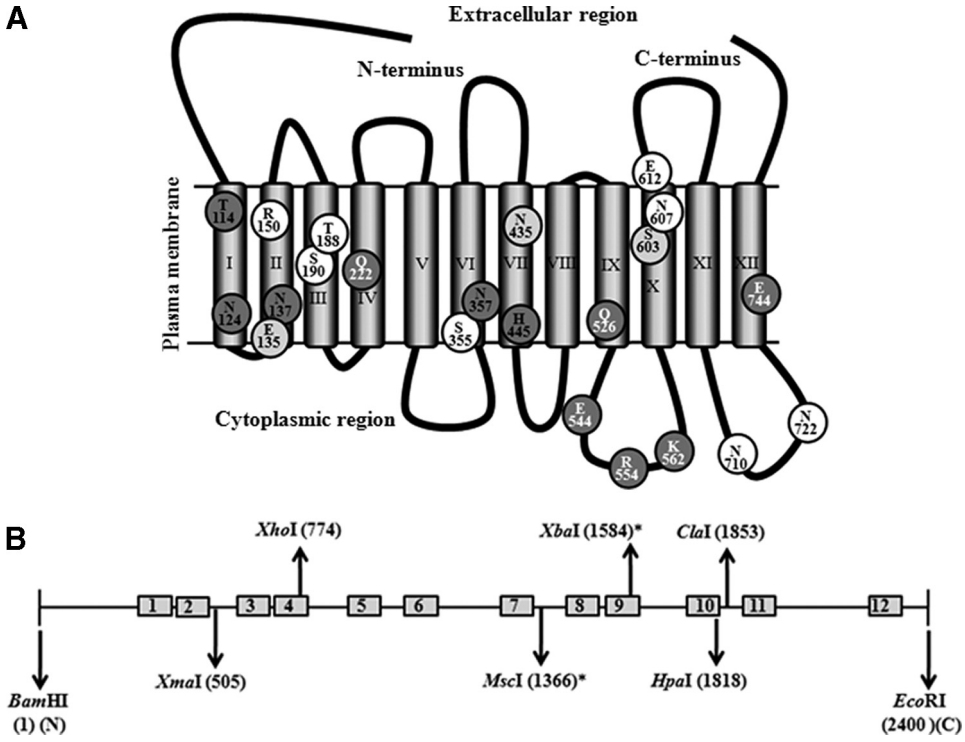

FIGURE 1. **Pictorial representation of putative Hgt1p topology showing the location of the charged/polar residues subjected to alanine scanning in the study (*A*) and restriction sites (*B*) in *HGT1*.** *A*, the topology model is based upon consensus generated using six different topology predicting software programs by Becker and co-workers (33) previously. The 12 transmembrane domains are shown as *rectangular bars*, and the residues subjected to alanine scanning in the study are marked as *circles* with residue identity and *number* inscribed in them. The residues are *shaded* to reflect the effect of alanine substitution on transport activity of Hgt1p (Table 2); residues *shaded dark gray with white letters* represent severe effect on transport activity (Group I), residues *shaded dark gray with black letters* represent moderate effect on the activity (Group II residues), residues *shaded light gray with black letters* represent mild effect on transport activity (Group III), and residues *shaded white with black letters* represent no to minor effect on the activity (Group IV). *B*, restriction sites used for genetic manipulation in construction of different clones in the study are marked by *arrows*, with the transmembrane domains depicted as *rectangular boxes with numbers*. The *asterisk* marks the restrictions sites introduced in *HGT1* gene as silent mutations.

Glutathione Transport Assay—met15Δhgt1Δ (ABC 817) strain transformed with different plasmid constructs bearing wild type or HGT1 mutants under the TEF promoter were grown in minimal media containing methionine and other supplements without uracil overnight. These cultures were reinoculated in the same media and allowed to grow till they reached exponential phase. Cells were harvested and washed and put on ice in a MES-buffered medium until the transport was initiated. Transport experiments were carried out with [^{35}S]GSH as described earlier (1). The results were expressed as nmol of glutathione·mg·protein^{-1}min^{-1}. For the measurements of total protein, 100 μl of the above cell suspension (cell suspension volume used for the transport assay) was boiled with 15% sodium hydroxide for 10 min followed by neutralization of total cell lysate by the addition of hydrochloric acid. 100 μl of this crude cell lysate was incubated with 0.1% Triton X-100 for 10 min, and total protein was estimated by using the Bradford reagent (Sigma) using bovine serum albumin as a standard.

Preparation of Cell Extract and Immunoblot Analysis—Total crude cell preparation and immunoblot analysis was done as described previously (25). Densitometry analysis of the unsaturated band signals was performed using the Scion Image software to quantify the protein expression levels in different mutants. The resulting signal intensity was normalized with respect to the band surface area (in square pixels) and expressed in arbitrary units. The relative protein expression levels in the mutant Hgt1p were represented as percentage expression relative to wild-type Hgt1p.

Cellular Localization of the Mutants by Confocal Microscopy—To localize Hgt1p and its different alanine mutants, indirect immunofluorescence was performed using a published protocol (26). Images were obtained with an inverted LSM510 META laser scanning confocal microscope (Carl Zeiss) fitted with a Plan-Apochromat ×100 (numerical aperture, 1.4) oil immersion objective. The 488-nm line of an argon ion laser was directed over an HFT UV/488 beam splitter, and fluorescence was detected using an NFT 490 beam splitter in combination with a BP 505–530 band pass filter. Images obtained were processed using Adobe Photoshop Version 5.5.

Sequence Analysis—The *HGT1* open reading frame and Hgt1p sequences were retrieved from the Saccharomyces genome data base. The multiple sequence alignment of the protein sequences was generated using ClustalX program using default parameters (27). For the prediction of transmembrane domains in Hgt1p, five different transmembrane prediction software programs were used: HMMTOP (28), TMHMM (29), MEMSAT (30), PHDHTM (31), and TopPRED II (32). The Hgt1p amino acid sequence was submitted as a query sequence, and predictions were made in default settings.

RESULTS

Selection of Amino Acid Residues in TMDs of Hgt1p for Alanine Scanning—A reasonably reliable topology model is a prerequisite for probing the role of amino acids in the transmembrane domains of Hgt1p. Previously, Becker and co-workers (33) predicted a topology model of Hgt1p with 12 transmembrane domains and extracellular N and C termini using topology prediction software in combination with multiple sequence alignment of the functionally characterized members of the OPT family (Fig. 1). Although the software predicted 14 transmembrane domains, the authors had omitted two of the predicted domains corresponding to the regions 537–568 and 707–724 citing the presence of conserved proline-rich motifs $EXLXGYX_2PG(R/K)PXAX_4KX_2G$ and $PPX(N/T)P$, respectively, in these regions. These motifs consist of proline residues in proximity to each other or a glycine residue, which theoretically disfavors a helix formation and, hence, were predicted to

TABLE 1
Polar/charged residues in the transmembrane domains of Hgt1p and residues selected for alanine scanning in this study

TMD	Polar/charged residue present in the domain	Residue mutated to alanine
TMD1 (109–127)	Thr-109, Thr-113, Thr-114, Asn-124, Gln-125	Thr-114, Asn-124
TMD2 (134–155)	Glu-135, Asn-137, Gln-142, Cys-145[a], Arg-150	Glu-135, Asn-137, Arg-150
TMD3 (179–200)	Thr-182, Thr-188, Ser-189, Ser-190, Thr-191, Asn-199	Thr-188, Ser-190
TMD4 (212–232)	Gln-214, Thr-220, Ser-221, Gln-222, Thr-232	Gln-222
TMD5 (277–296)	Ser-285	
TMD6 (354–374)	Ser-355, Asn-357, Thr-358, Ser-361, Cys-372[a]	Ser-355, Asn-57
TMD7 (427–449)	Ser-427, Ser-431, Asn-435, His-445, Cys-446[a]	Asn-435, His-445
TMD8 (483–502)	Gln-489, Cys-501[a], Cys-502[a]	
TMD9 (509–529)	Ser-519, Asn-522, Gln-526	Gln-526
Loop (537–568)	Asn-540, Thr-543, Glu-544, Cys-547, Arg-554, Asn-558, Lys-562	Glu-544, Arg-554, Lys-562
TMD10 (591–613)	Gln-596, Thr-600, Ser-603, Asn-607, Gln-611, Glu-612	Ser-603, Asn-607, Glu-612
TMD11 (661–679)	Gln-679	
Loop (707–724)	Thr-707, Asn-710, Ser-712, Ser-718, Cys-720[a], Asn-722	Asn-710, Asn-722
TMD12 (739–759)	Glu-744, Ser-750, Cys-757[a], Gln-759	Glu-744

[a] The cysteine residues have been subjected to mutagenesis analysis in an independent study (9).

form loops in the predicted topology model (33). We have carried out an independent topology prediction analysis using also additional membrane protein topology prediction software reported in the literature. Our analysis leads us to concur with the Becker topology model of Hgt1p with the 12 transmembrane domains (data not shown). Hence, the predicted topology model has been used as a platform for the structure-functional analysis of Hgt1p. However, in the absence of any firm experimental evidence for excluding the two likely transmembrane domains spanning the regions 537–568 and 707–724 in Hgt1p, we have included these regions for our mutational study, while staying with the Wiles *et al.* (33) topology model of Hgt1p.

In the absence of any previous hints on the important motifs or conserved amino acids in the transmembrane domains of Hgt1p (or any other member of the OPT family) that could be involved in substrate recognition, we adopted a comprehensive approach to identify the important residues or domains in Hgt1p that may play a specific role in substrate translocation. Glutathione, the substrate for Hgt1p, is a hydrophilic substrate, and prior studies on structural characterization of transporters of the other hydrophilic substrates have established that transmembrane domains lining the channels are rich in charged and polar residues. An examination of the 12 predicted transmembrane domains of Hgt1p revealed that each of these domains had at least one charged/polar residue in it, resulting in a total of 49 residues (Table 1). As the charged and polar residues that form a part of the permeability channel show a characteristic distribution where they often tend to cluster on one face of the helix (amphiphatic arrangement), helix wheel projections were drawn for each of the 12 transmembrane domains (supplemental Fig. 1). These helix wheel projections were analyzed for the presence and distribution of the charged and polar residues in these domains (supplemental Fig 1 and Table 1). Two of the 12 transmembrane domains (TMD 5 and TMD11) contained only a single polar residue, and hence, were not included in this study. TMD8 contains three polar residues, Gln-489, Cys-501, and Cys-502. However, the two cysteine residues in TMD8 are not crucial for the functional activity of Hgt1p (9), and hence, the TMD8 was also not included in our mutational analysis of Hgt1p. Of the remaining 9 transmembrane domains, TMDs 1, 2, 4, 6, 7, 9, 10, and 12 have a clear distinction between the polar and nonpolar phase, and TMD3 is very rich in polar residues, which are scattered all around the helix. Hence, from these nine transmembrane domains, all the five charged residues in the predicted transmembrane domains (Glu-135, Arg-150, His-445, Glu-612, and Glu-744) were selected for mutational analysis in this study. With the remaining polar residues in the transmembrane domains, the following two criteria were used to select the residues; (*a*) restriction was made with respect to number of residues, selecting one or. at the most. two residues from each transmembrane domains so as to cover all the remaining nine transmembrane domains in Hgt1p, and (*b*) when picking more than one polar residue in a transmembrane domain, residues present in different faces of the helices were selected.

In addition, three of the highly conserved charged residues, Glu-544, Arg-554, and Lys-562, were selected from the region spanning 537–568, and two polar residues (Asn-710 and Asn-722) were selected from the region spanning 707–724. Thus a total of 22 amino acids representative of 9 transmembrane domains of Hgt1p and 2 intracellular loops were mutagenized to the alanine residue and evaluated for the functional activity (Fig. 1 and Table 1).

Functional Evaluation of the Alanine Mutants of Hgt1p—A preliminary characterization of the alanine mutants of Hgt1p was done using a plate-based dual complementation-cum-toxicity assay, previously designed for the rapid evaluation of the functional activity of the mutants of the transporter (9). Briefly, the assay is based upon the dual behavior of Hgt1p, expressed from TEF promoter in a *met15*Δ*hgt1*Δ strain, an organic sulfur auxotroph defective in glutathione uptake. While at low glutathione concentrations (15 μM or lower), *HGT1* expressed under the TEF promoter complements the growth defect in a *met15*Δ*hgt1*Δ strain very well (1), the same construct results in toxicity when cells are grown in medium containing 30 μM or higher glutathione concentrations (34). Thus, the assay is used to evaluate the functional activity of Hgt1p with respect to two parameters. (*a*) ability to complement the GSH transport defect of the strain *met15*Δ*hgt1*Δ at low concentrations of GSH and (*b*) the ability to cause toxicity in media containing higher concentrations of GSH.

The plasmids bearing wild-type Hgt1p or with the mutated residue in Hgt1p were individually transformed into the *met15*Δ*hgt1*Δ strain (ABC 817) and checked for growth by dilution spotting on minimal media containing a range of glutathione concentrations as the sole source of organic sulfur (Fig. 2). Functional evaluation of the mutations in Hgt1p using the plate assay identified four subgroups, (*a*) severe effect (complemen-

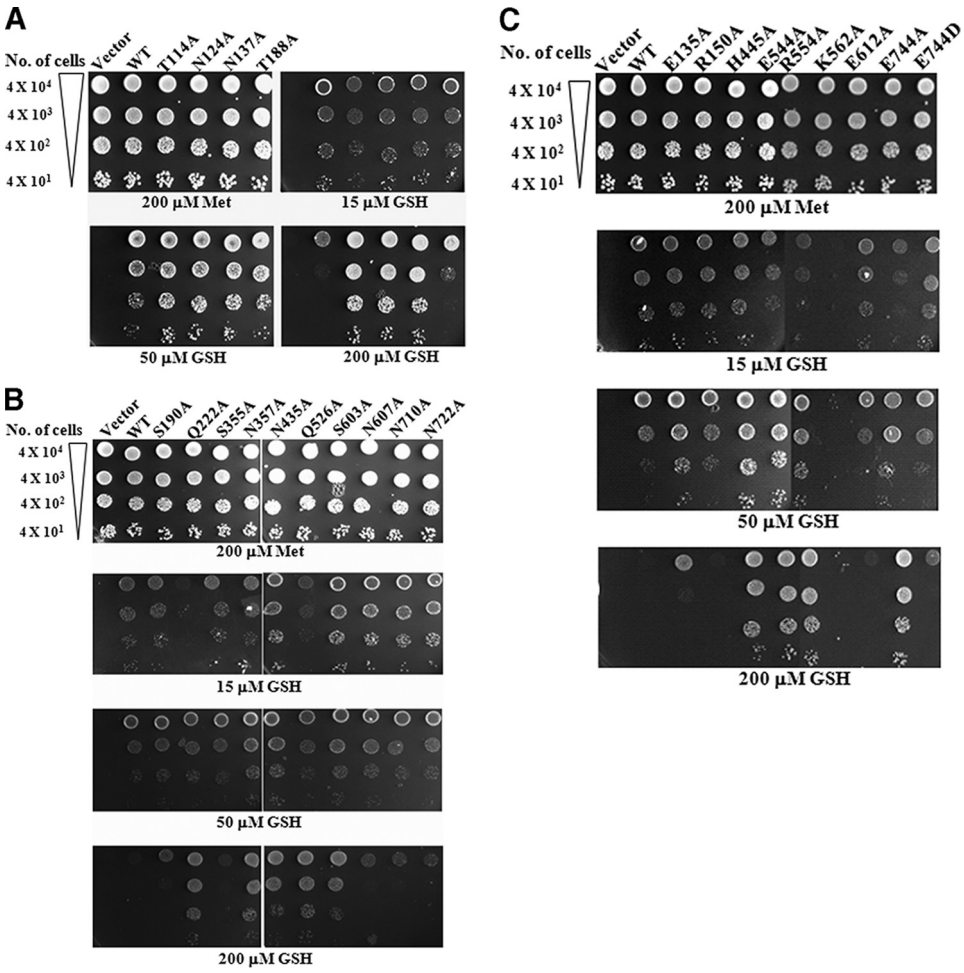

FIGURE 2. **Functional characterization of alanine mutants of the polar/charged residues in the putative transmembrane domains of Hgt1p.** The *met15*Δ*hgt1*Δ strain (ABC 817) was transformed with wild-type (*WT*) Hgt1p and the different alanine mutants of Hgt1p expressed under the TEF promoter along with control vector (p416M1-TEF) and used for plate-based dual complementation-cum-toxicity assay by dilution spotting on minimal media containing different concentration of glutathione as described under "Experimental Procedures." The functional analysis of the alanine mutants of polar residues is shown in *A* and *B* and, for the charged residues, in *C*.

tation-defective at 15 μM GSH, no toxicity at higher GSH concentrations; those mutants showing significant loss in activity as reflected by loss in ability to complement *hgt1*Δ defect at low glutathione concentrations), (*b*) moderate effect (complementation-positive at 15 μM GSH, no toxicity at higher GSH concentrations; mutants that permitted growth at higher glutathione concentration, *i.e.* no toxicity is observed in the cells transformed with these set of mutants), (*c*) mild effect (complementation-positive at 15 μM GSH, mild toxicity at higher concentrations; mutants showing decreased toxicity, with growth observed at glutathione concentrations higher then 100 μM, unlike the wild type Hgt1p, for which toxicity sets in at 30 μM glutathione), and (*d*) very mild to no effect (complementation-positive at 15 μM GSH and severe toxicity at higher concentrations; mutants which behave very similar to the wild-type protein in terms of their ability to complement the *met15*Δ*hgt1*Δ strain (ABC 817) or cause severe toxicity to the cells (Table 2)).

To corroborate these spotting assays with actual transport data, we measured the initial rate of [^{35}S]glutathione uptake in the *met15*Δ*hgt1*Δ strain (ABC 817) transformed with the alanine mutants of Hgt1p (Table 2). Interestingly, the quantitative information generated from the biochemical assay also defined four groups of activity which correlated closely with the plate assay; (*a*) those with severe effect showed <20% that of the activity compared with the wild-type protein, (*b*) those with moderate effect fell into roughly 20–30% activity bracket, (*c*) those with mild effect retained nearly 50% activity, and (*d*) those with very mild to no effect showed >75% activity. The only exception in this grouping was the N124A mutant, which despite showing complementation ability comparable with wild-type Hgt1p, exhibited only 16% transport activity; nonetheless, it was placed in Group II based upon its behavior in the plate based dual-complementation assay. Furthermore, as the plate assay generated a reliable picture of the activity of the different mutants, we did not determine the [^{35}S]glutathione uptake activity for all the mutants that fell into the last group.

Among the 22 amino acids initially selected, we were able to identify 11 residues in the different transmembrane domains of Hgt1p, which when replaced by a relatively inert residue (alanine) resulted in a significant decline in glutathione uptake ability of the protein. Six of these residues led to severe defect in transport ability of Hgt1p, and these residues were located in TMD4 (Gln-222), TMD9 (Gln-526), the intracellular loop between TMD9 and TMD10 (Glu-544, Arg-554, Lys-562) and TMD12 (Glu-744). In contrast, five of the residues located in TMD1 (Thr-114, Asn-124), TMD2 (Asn-137), TMD6 (Asn-357), and TMD7 (His-445) led to a moderate effect on the functional efficiency of Hgt1p upon being mutated to alanine. To define the role of these residues in the function of Hgt1p, we undertook a detailed biochemical characterization of these 11 mutants.

Evaluation of the Protein Expression Levels of Alanine Mutants of Hgt1p Reveals That Only T114A Shows a Significant Reduction in Protein Levels—The decreased activity of the alanine mutants of Hgt1p observed using whole cell-based growth or transport assay can be attributed either to decreased expression levels of the protein, a defect in trafficking to the cell surface, or loss in the functional activity of the protein *per se*. The protein expression levels of the Hgt1p mutants were measured by immunoblotting. Equal amounts of the crude protein extracts prepared from the *met15*Δ*hgt1*Δ strain (ABC 817)

TABLE 2

Grouping of the alanine mutants of Hgt1p based upon their effect on the functional activity of the transporter using dual complementation-cum-toxicity assay and percentage transport activity

The mutants were analyzed for the functional activity using the plate-based assay categorized into four groups based upon their activity in terms of their ability to complement *met15*Δ*hgt1*Δ strain (ABC 817) at low concentrations of glutathione and cause toxicity to the cells at glutathione concentrations higher than 50 μM. For quantification of the functional activity of the mutants, the initial rate of uptake of glutathione (100 μM) was measured in *met15*Δ*hgt1*Δ strain (ABC 817) as described under "Experimental Procedures." The results were normalized to the rate of glutathione uptake measured for the wild-type Hgt1p (54.5 ± 4.3 nmol $min^{-1}mg{\cdot}protein^{-1}$). Data were obtained from two independent experiments done in triplicate and are represented as percentage activity relative to wild-type Hgt1p and expressed as the mean ± S.E. Visual scoring symbols: +, yes; +/−, mild; −, no. ND, not determined.

Mutant (TMD)	Complementation (15 μM GSH)	Toxicity (>50 μM GSH)	Transport activity (mean ± S.E.)
WT-Hgt1p	+	+	100.0 ± 1.6
			%
Severe effect-Group I			
Q222A (TMD 4)	−	−	9.2 ± 0.6
Q526A (TMD 9)	−	−	19.2 ± 0.0
E544A (ICL9–10)	+/−	−	20.8 ± 0.1
R554A (ICL9–10)	+/−	−	18.7 ± 0.1
K562A (ICL9–10)	−	−	1.4 ± 0.0
E744A (TMD 12)	−	−	6.2 ± 0.0
Moderate effect-Group II			
T114A (TMD 1)	+	−	26.5 ± 0.1
N124A (TMD 1)	+	−	15.6 ± 0.7
N137A (TMD 2)	+	−	22.7 ± 0.5
N357A (TMD 6)	+	−	28.3 ± 1.8
H445A (TMD 7)	+	−	25.7 ± 1.5
Mild effect-Group III			
E135A (TMD 2)	+	+/−	57.2 ± 1.6
N435A (TMD 7)	+	+/−	47.6 ± 1.9
S603A (TMD 10)	+	+/−	69.1 ± 4.5
No to minor effect-Group IV			
R150A (TMD 2)	+	+	ND
T188A (TMD 3)	+	+	89.8 ± 6.2
S190A (TMD 3)	+	+	76.1 ± 7.2
S355A (TMD 6)	+	+	ND
N607A (TMD 10)	+	+	ND
E612A (TMD 10)	+	+	89.4 ± 3.2
N710A (ICL11–12)	+	+	ND
N722A (ICL11–12)	+	+	ND

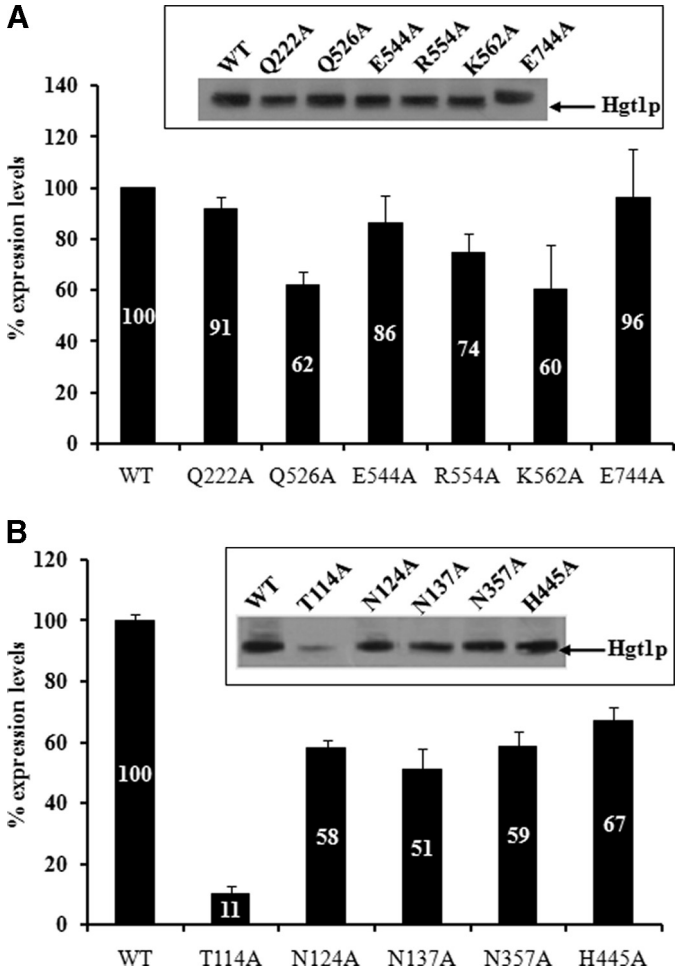

FIGURE 3. **Quantification of the total protein expression levels of alanine mutants of Hgt1p showing severe effect on activity (Group I mutants) (*A*) and moderate effect on activity (Group II) (*B*).** The crude extracts prepared from the *met15*Δ*hgt1*Δ strain (ABC 817) transformed with plasmids bearing the different alanine mutants of Hgt1p were prepared, and ~20 μg of total protein was resolved using 9% SDS-PAGE, electroblotted to a nitrocellulose membrane. The blot was probed with mouse anti-HA (Cell Signaling) at 1:1000 dilution as primary antibody and goat anti-mouse IgG horseradish peroxidase-conjugated antibody (Cell Signaling, at 1:2500 dilution) as secondary antibody. The signal was detected using ECL kit (Amersham Biosciences). Molecular weight markers (SM0431, MBI Fermentas) were used to estimate the protein molecular weight. The total protein was quantified by densitometry analysis of protein bands. The data are expressed as percentage protein expression normalized to the wild-type (*WT*) expression level and are the mean of the protein expression levels obtained in three independent experiments. A representative blot is shown in the *inset*. Equal loading of the proteins (20 μg) in each well of the gel was visually monitored by Coomassie staining of a duplicate gel and Ponceau S staining of the membrane after transfer (data not shown).

transformed with the plasmids bearing the alanine mutants of Hgt1p were loaded onto the SDS-PAGE gels, electroblotted to the membrane, and probed with anti-HA monoclonal antibody. As shown in Fig. 3, an 85-kDa band corresponding to the wild-type Hgt1p was visualized for all the mutants, although the mutants showed variation in the expression levels. Densitometry analysis of unsaturated band signals revealed that in particular T114A mutant showed a drastic fall in protein expression levels, suggesting that the residue might be crucial for protein folding and stability (Fig. 3). However, for the other mutants, the protein expression levels did not appear to be significantly altered. The protein expression levels ranged between 50 and 90% relative to the wild-type protein levels, indicating that these mutants did not significantly perturb the protein structure and stability, and the significant loss in glutathione uptake ability of these mutants was not a consequence of decreased protein stability and protein expression levels.

Analysis of Cell Surface Trafficking of Mutants with Loss in Functional Activity Reveals E744A Is Defective in Trafficking—Hgt1p is a plasma membrane-localized transporter, and localization studies with Hgt1p expressed from its native promoter as well as from the constitutive TEF promoter has revealed exclusive plasma membrane localization for the transporter (9). As any mutation that affects trafficking could also explain the loss in functional activity, we examined all 11 mutants expressed from the TEF promoter for their subcellular localization by indirect immunofluorescence using anti-HA monoclonal antibody. A very robust signal was observed at the cellular periphery for the cells transformed with wild-type Hgt1p as well as for the majority of the mutants (N124A, N137A, N357A, H445A, Q222A, Q526A, E544A, R554A, K562A) (Fig. 4). Among these, K562A also showed a small amount of intracellular signal in addition to the cell surface signal in few of the

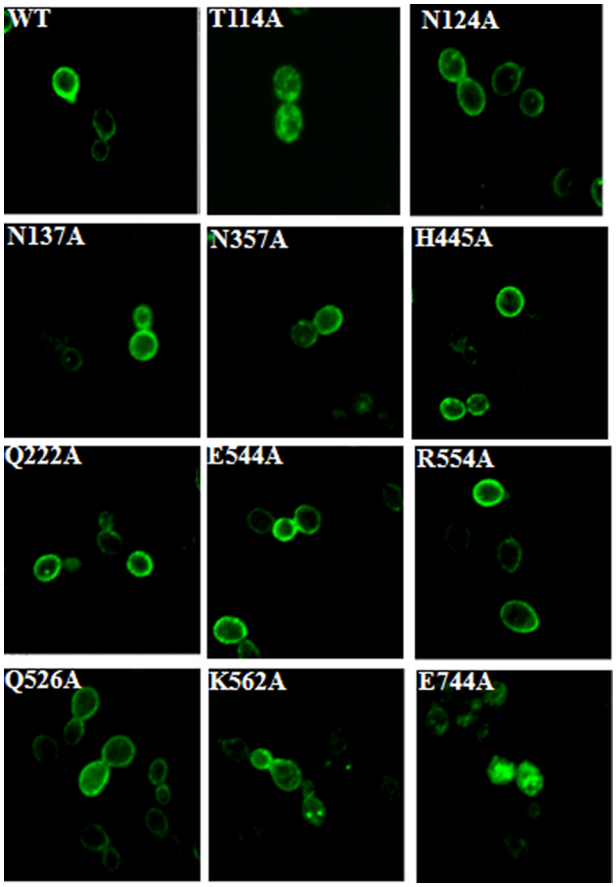

FIGURE 4. **Cell surface localization of alanine mutants of Hgt1p showing a severe effect on activity (Group I mutants) and moderate effect on activity (Group II).** The strain *met15Δhgt1Δ* (ABC 817) was transformed with plasmids bearing the different alanine mutants of Hgt1p and labeled by indirect immunofluorescence using mouse anti-HA (Cell Signaling) primary antibody (at 1:100 dilution) and goat anti-mouse IgG horseradish peroxidase-conjugated antibody (Cell Signaling) secondary antibody (at 1:500 dilution) and visualized using confocal microscope, as described under "Experimental Procedures." Only fluorescence images have been shown. *WT*, wild type.

cells, suggesting a partial defect in trafficking of the mutant. However, very poor cell surface signal was detected for T114A and E744A mutant. The staining pattern for E744A suggested that the protein was trapped in the endoplasmic reticulum. These findings suggest that replacement of Glu-744 residues with alanine interfered with the trafficking of the protein to the cell surface, and this may be the principal reason for the observed loss in functional activity of the mutant.

In the case of T114A a diffused and relatively weak cytosolic signal was observed, which probably reflects the decreased protein expression levels observed earlier for this mutant in the Western blot. These findings further confirm that loss in activity of the T114A mutant is mainly a consequence of decreased protein expression levels.

Kinetic Analysis of the Mutants Reveals a Critical Role of Asn-124 (TMD1), Gln-222 (TMD4), and Gln-526 (TMD9) in Glutathione Transport by Hgt1p—The analysis of total protein expression levels and cell surface localization of the mutants in Group I and Group II revealed that with the exception of T114A and E744A, the remaining mutations did not bear a significant effect on the protein expression or its cell surface localization. This suggests that loss in functional activity of these mutants might be because of some specific defect related to the ability of the mutants to transport glutathione. Hence, to characterize these residues for their role in substrate binding or translocation, we undertook the measurement of kinetic parameters of the mutants by measuring the initial rates of glutathione uptake over a range of glutathione concentrations. As K562A and E744A had very poor activity, these could not be included for the kinetic study. The apparent K_m and V_{max} values and the K_m/V_{max} ratios (transport efficiencies) obtained for the rest of the mutants are summarized in Table 3. The K_m and V_{max} values for wild-type Hgt1p were estimated to be 48.1 ± 10.5 μM and 57.8 ± 3.9 nmol of glutathione·mg·protein^{-1}min^{-1}. Although the K_m was in close agreement with the previously reported value (53.8 ± 5.5 μM), the V_{max} differed significantly from the previously reported value (10.0 ± 0.6 nmol of

TABLE 3

Kinetic characterization of the mutant showing severe/moderate loss in activity; estimation of the kinetic parameters and normalization to the protein expression levels

The initial rate of glutathione uptake was measured at glutathione concentrations ranging from 0.0125 to 0.4 mM by harvesting cells incubated with radiolabeled glutathione at 30- and 180-s time intervals. After subtracting the initial rate of glutathione uptake in vector-transformed *met15Δhgt1Δ* strain (ABC 817) from the initial rate of glutathione uptake in the different test construct-transformed yeast cells, initial rates of glutathione uptake corresponding to Hgt1p were calculated. The experiment was repeated a minimum of two times for each mutant in duplicate at each glutathione concentration. The average K_m and V_{max} values were determined by nonlinear regression analysis of *V versus* [*S*] graphs showing saturation kinetics using GraphPad Prism Version 5.01 software. NM, not measurable.

Mutant (TMD)	Protein expression	Kinetic parameters		Corrected V_{max} [a]	Corrected V_{max}/K_m
		K_m	V_{max} [a]		
	%	μM		nmol of glutathione·mg·protein^{-1}min^{-1}	nmol of glutathione·mg·protein^{-1}min^{-1}μM^{-1}
WT-Hgt1p	100	48.1 ± 10.5	57.8 ± 3.9		1.2
Severe effect (complementation defective)					
Q222A (TMD4)	91	213.9 ± 69.5	11.4 ± 1.9	12.5	0.1
Q526A (TMD9)	62	372.3 ± 106.7	38.0 ± 6.5	61.3	0.2
E544A (ICL9–10)	86	85.2 ± 25.1	10.5 ± 1.2	12.2	0.1
R554A (ICL9–10)	74	116.6 ± 53.1	16.5 ± 3.1	22.3	0.2
Moderate effect (no toxicity)					
T114A (TMD1)	11	40.2 ± 19.0	8.3 ± 1.1	75.5	1.9
N124A (TMD1)	58	NM	NM		
N137A (TMD2)	51	29.3 ± 17.0	21.7 ± 3.3	42.5	1.5
N357A (TMD6)	59	24.3 ± 11.6	19.6 ± 2.3	33.2	1.4
H445A (TMD7)	67	28.5 ± 11.1	23.6 ± 2.4	35.2	1.2

[a] V_{max} was adjusted to the protein expression levels.

glutathione·mg·protein^{-1}min^{-1}) (1). The difference in the V_{max} is likely to be a consequence of growing the yeast cells in medium additionally supplemented with adenine, leucine, tryptophan, and lysine (in addition to the required supplements histidine and methionine). This medium leads to significantly better growth that could have resulted in better protein expression. As K_m is an intrinsic property of the protein whereas V_{max} can vary with the protein expression levels and experimental conditions, the results were considered to be reliable and used for evaluation of the mutants.

The kinetic characterization of the mutants revealed interesting insights into the roles of residues in the functional activity of the transporters. In particular, the Q526A mutant in TMD9 showed a nearly 8-fold increase in its K_m for glutathione, with the corrected V_{max} value nearly the same as the wild-type V_{max} value, thereby resulting in nearly a 7-fold decrease in the transport capacity. A nearly 4-fold increase in K_m for glutathione was also observed for another glutamine residue, Gln-222, in TMD4. However, Q222A also exhibited a significant loss in corrected V_{max} value such that the transport efficiency of the mutant Hgt1p fell by nearly 20-fold. The significant decrease in affinity for glutathione upon mutation of the Gln-222 and Gln-526 to alanine suggests these residues play a critical role in interacting with the substrate.

In contrast, the kinetic analysis of E544A and R544A revealed that mutant yielded a nearly 2-fold increase in K_m values but a drastic loss in the catalytic activity. The corrected V_{max} values for E544A and R554A mutants were 12.2 and 22.3 nmol of glutathione·mg·protein^{-1}min^{-1}, respectively, resulting in a nearly 8- and 6-fold decrease in transport efficiency of the mutants. The decreased V_{max} values obtained for the three mutants, Q222A, E544A, and R554A, which could not be attributed to the decreased protein levels for the mutants, suggest that these residues might play some critical role in the conformation changes associated with translocation of the substrate by the protein or, alternatively, in binding of protons to drive the translocation of the substrate.

Among the mutants that were moderately affected in activity (Group II, Table 2), T114A showed a drastic fall in its V_{max} value, which was in agreement with its decreased protein expression a level. In contrast, mutants N137A, N357A, and H445A showed a nearly 2-fold decrease in K_m and corrected V_{max} values such that the transport efficiency for these mutants remained nearly similar to the wild type. Considering the observed alterations in the kinetic parameters for these three mutants, it appears likely that these residues are not directly involved in interacting with the substrate. Instead, the introduction of alanine at these positions most likely leads to minor conformation changes in the transporter leading to decreased protein stability and, hence, protein expression levels and indirectly affects the substrate binding.

In contrast, the N124A mutant showed non-saturating binding even at 400 μM glutathione concentration, making it difficult to obtain a reliable estimate of the kinetic parameters of the mutant. Moreover, the initial rate of glutathione uptake at different concentration was marginally more than the background values (measured in the vector transformed cells), implying a significant defect in the substrate binding or translocation mechanism of the protein for this particular mutant.

Functional Analysis of K562R and K562L Reveals the Lysine Residue Is Mandatory at Position 562 in Hgt1p—The drastic fall in activity of K562A, which otherwise exhibited total and surface protein expression levels comparable with the wild-type Hgt1p, suggested that this residue might play an important role in the transport activity of the protein. As the kinetic parameters could not be measured for this mutant, we tried to further probe the importance of this residue by construction and functional evaluation of K562L and K562R mutants. By substitution of Lys-562 with a conservative residue (Arg) and a non-conservative residue (Leu), we hoped to distinguish between the requirement for positive charge and/or steric (side-chain volume) properties at the position 562 for the transport activity of Hgt1p.

As shown in Fig. 5, replacement of Lys-562 either with positively charged Arg or iso-steric Leu led to drastic loss in the protein activity. The K562L, like K562A mutant, failed to complement the *hgt1*Δ defect of *met15*Δ*hgt1*Δ strain (ABC 817) even at as high as 200 μM GSH and exhibited virtually no glutathione uptake activity in the radiolabeled GSH assay (Fig. 5, *A* and *B*). In contrast, K562R exhibited very poor complementation ability, with the mutated protein supporting growth of *met15*Δ*hgt1*Δ strain (ABC 817) at 50 μM or higher glutathione concentrations only, and no toxicity was observed (Fig. 5*A*). The poor activity of the mutant was also reflected in the quantitative assay, where it recorded only 8–12% GSH uptake ability relative to the wild-type protein at 100 μM GSH (Fig. 5*B*). Radiolabeled GSH uptake assay of K562R at higher GSH concentrations (400 μM GSH) also failed to exhibit any significant glutathione uptake into the cells (data not shown). An examination of the total protein expression levels (data not shown) and cell surface expression levels (Fig. 5*C*) revealed that the observed loss in activity of the mutants could not be attributed to defective protein expression levels or trafficking.

Thus, the complete lack of activity of the K562A/L mutants coupled with the inability of a positively charged residue (Arg) to efficiently compensate for the lysine residue at position 562 suggests that presence of lysine *per se* is mandatory for the functional activity of the transporter. Furthermore, the lack of transport capability of K562R even at high GSH concentrations implies that Lys-562 could be a key catalytic residue during the substrate translocation process of the transporter.

Conservation Pattern of Residues Important for Hgt1p Function by Multiple Sequence Alignment with Other Oligopeptide Transporters—Comparative sequence analysis can yield valuable insights into the functional significance of a residue. Hence, it was of interest to examine the status of the critical residues found essential for the functional activity of Hgt1p in the other peptide transport (PT) members, which have been characterized in terms of their substrate specificity.

The OPT family contains two distinct clades, the peptide transporting (PT) clade and the yellow stripe (YS) clade that are only remotely related to each other and are distinguished on the basis of their substrate specificity and phylogenetic analysis (3). The PT clade that contains 205 members, including Hgt1p, has only four other members for which

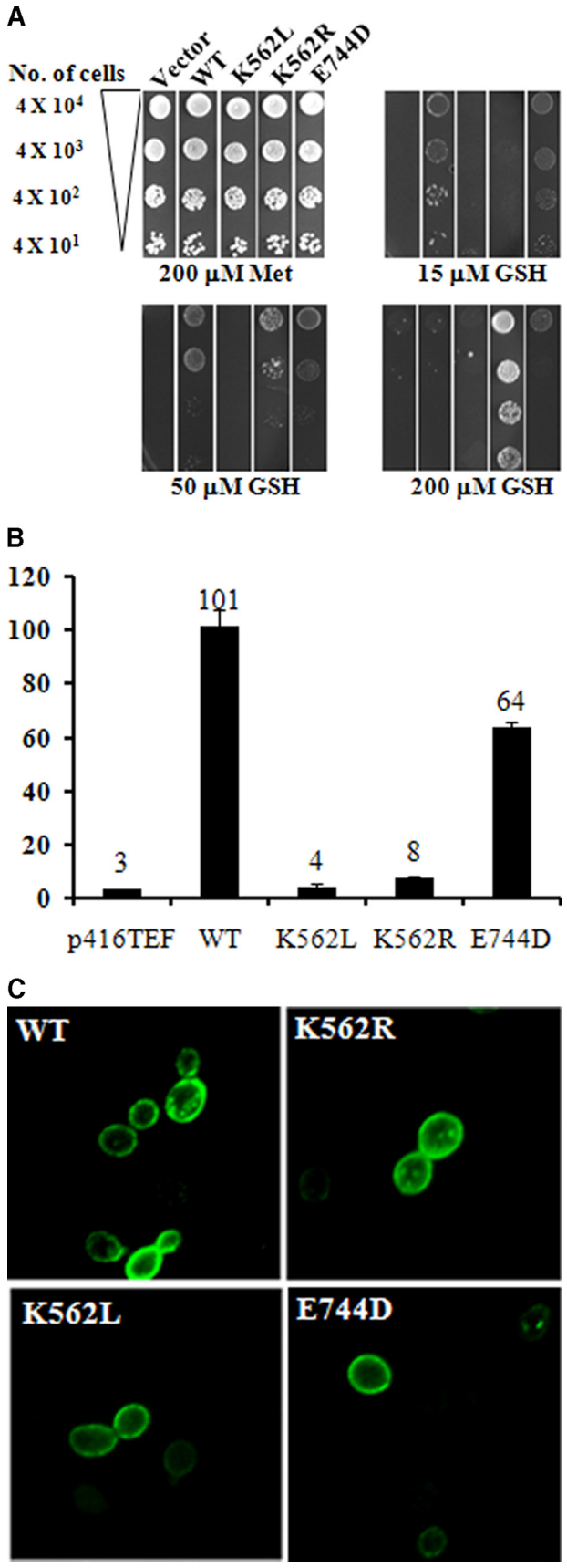

FIGURE 5. **Functional analysis of K562L, K562R, and E744D mutants reveal significant loss in activity for K562L and K562R mutants.** *A*, the strain *met15*Δ*hgt1*Δ (ABC 817) was transformed with plasmids bearing the K562L, K562R, and E744D mutations in Hgt1p and used for plate-based dual complementation-cum-toxicity assay by dilution spotting on minimal media containing different concentrations of glutathione as described under "Experimental Procedures." *B*, measurement of the rate of radiolabeled glutathione uptake. The data are represented as percentage of rate of uptake by the mutants relative to wild-type Hgt1p (*WT*). The rate of GSH uptake in wild-type Hgt1p was 38.1 ± 2.8 nmol min^{-1}mg·$protein^{-1}$. Experiments were repeated twice, in triplicate, and representative data are shown as the mean ± S.D. *C*, cell surface localization analysis by indirect immunofluorescence using mouse anti-HA (Cell Signaling) primary antibody (at 1:100 dilution) and goat anti-mouse IgG horseradish peroxidase-conjugated antibody (Cell Signaling) secondary antibody (at 1:500 dilution). Cells were visualized using confocal microscope, as described under "Experimental Procedures." Only fluorescence images have been shown.

physiological substrate preference have been clearly established. These include Pgt1, CaOpt1, Isp4, and AtOpt4. Pgt1 has been recently characterized as a high affinity glutathione transporter from *Schizosaccharomyces pombe* (4), whereas AtOpt4 from *Arabidopsis thaliana*, CaOpt1 from *Candida albicans*, and Isp4 from *S. pombe* have been shown to specifically mediate uptake of oligopeptides (7, 35, 36).

Multiple sequence alignment of these five PT family members revealed a number of polar/charged residues conserved across the PT members within the predicted transmembrane domains (Fig. 6). Interestingly, four of the six residues, Asn-124 (TMD1), Gln-222 (TMD4), and Glu-544 and Lys-562 (ICL 537–568) identified to be crucial for the substrate translocation are completely conserved among the five PT members. The high degree of conservation of Asn-124, Gln-222, Glu-544, and Lys-562 among the evolutionary distant members of the PT member suggests that these key residues could be important for the catalytic activity of the PT clade transporters in general. In contrast to the high degree of conservation of Gln-222 across the PT members, Gln-526 in TMD9, the only residue which exhibited a significant increase in K_m for GSH without any significant effect on V_{max} was conserved only among the glutathione transporters (Hgt1p and Pgt1).

The mutants R554A and E744A (TMD12), which exhibited a significantly decreased transport activity, displayed a complete conservation of positive and negative charge conservation at the respective positions in the five OPT members (Fig. 6). In the case of Glu-744, sequence alignment revealed that the glutamate residue was found exclusively in Hgt1p and was not conserved among the other members. Even the *S. pombe* glutathione transporter lacked Glu-744 and contained an Asp at this residue, like the other oligopeptide transporter members. As the drastic loss in activity of E744A mutant was attributed to the entrapment of the mutant transporter in endoplasmic reticulum, we investigated the residue further in the light of the sequence analysis. We created an E744D mutation and evaluated it for functionality. The E744D mutant, unlike E744A mutant, exhibited functionality like the wild-type protein, as seen from the plate assay, and exhibited around 65% transport activity in the radiolabeled GSH assay (Fig. 5, *A* and *B*). The E744D mutant was also able to traffic to the cell surface efficiently, further underlining the requirement for a negative charge at the amino acid position corresponding to 744 in Hgt1p among the PT members.

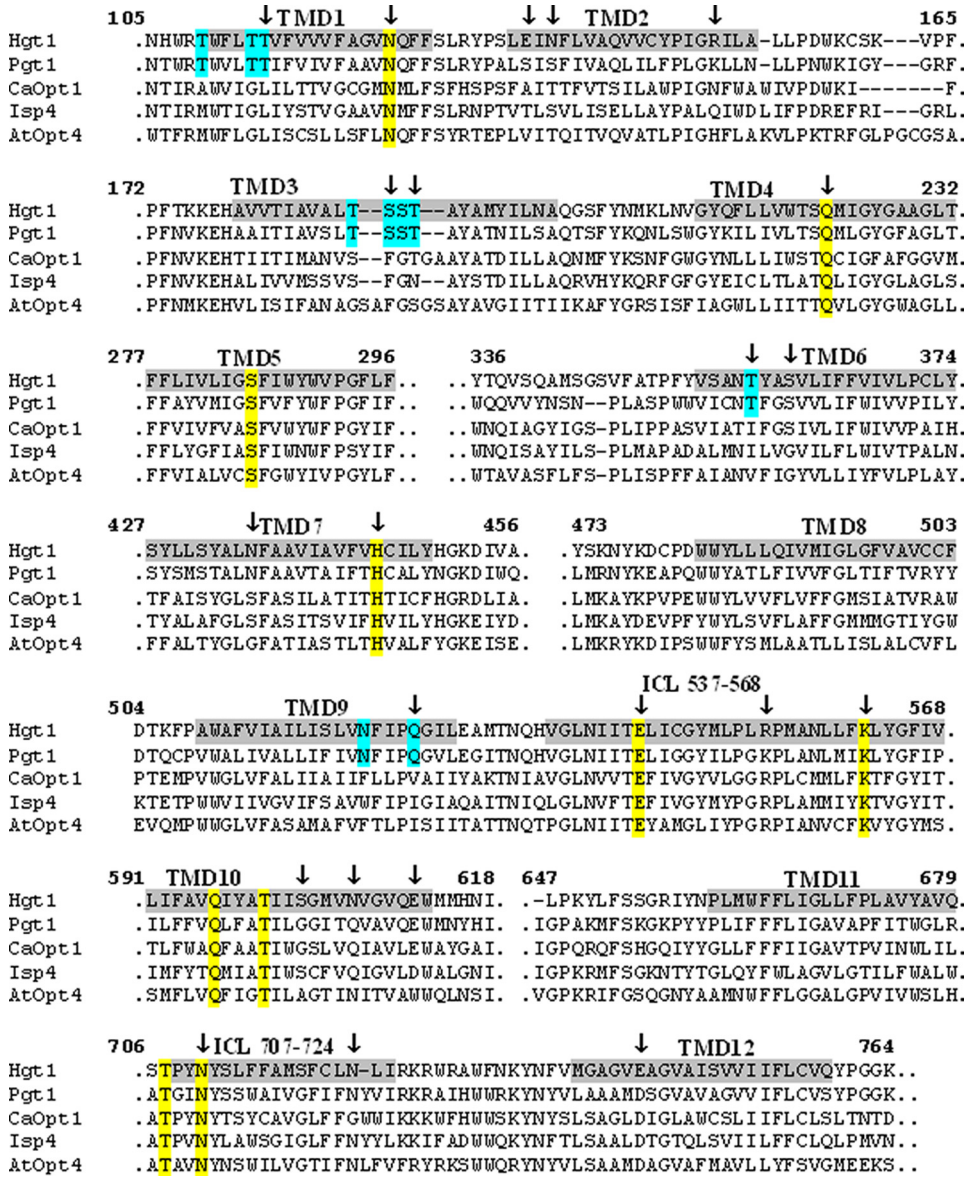

FIGURE 6. **Multiple sequence alignment for the protein sequences of the 5 PT members with defined substrate specificity.** Sequences of Hgt1 (gi 6322249), Pgt1 (gi 19115899), CaOpt1 (gi 2367386), Isp4 (gi 1827508), and AtOpt4 (gi 15237689) were retrieved from Entrez at the NCBI website and aligned using ClustalX program (27). The sequence alignment has been edited to show only the 12 putative transmembrane domains in Hgt1 and the two putative transmembrane domains, excluded in the Becker's group topology (33) (*shaded gray*). The numbers corresponding to amino acids sequence of Hgt1 have been shown. The conserved polar and charged residues are *shaded yellow*, and the residues conserved in the glutathione transporters (Hgt1 and Pgt1), although absent in non-glutathione transporters, are *shaded cyan blue*. The residues subjected to alanine scanning in this study are marked with an *arrow*.

DISCUSSION

The OPT transporter family catalyzes the uptake of oligopeptides or peptide-like substrates such as metal-secondary amino acid conjugates or glutathione in a proton-dependent manner (3, 7). However, how the transport occurs, the TMD helices, and the residues involved in either the recognition or the translocation process are not known and have not been investigated. A systematic effort was, therefore, initiated in this study for the first time to obtain insights into this process in this large, uncharacterized family of transporters.

Hgt1p, the high affinity glutathione transporter of *S. cerevisiae*, the best studied member of this family (1, 7, 8, 34, 37), seemed ideally suited to yield insights with a simple plate assay (9) and the ready availability of glutathione and radiolabeled glutathione (in contrast to other substrates of the OPT members). The substrate of Hgt1p, glutathione, is hydrophilic in nature, and therefore, charged and polar residues within the transmembrane domains appeared to be logical candidates for participating in the substrate binding and translocation while also possibly playing other structurally significant roles. This assumption has been the basis of our strategy for selecting a set of 22 polar and charged amino acids across the predicted transmembrane domains in Hgt1p for alanine mutagenesis in this study.

A detailed functional analysis of these residues has revealed that mutation of several of these residues to the nonpolar residue alanine led to a drastic reduction of activity. Those showing a significant effect were found in TMD1 (Thr-114, Asn-124), TMD4 (Gln-222), and TMD9 (Gln-526), implying these as clearly very important domains for the functional activity of Hgt1p. An examination of the helix wheel projection of these transmembrane domains shows that whereas Thr-114 and Asn-124 in TMD1 and Gln-526 in TMD9 clearly tend to cluster with the other hydrophilic residues in the domain, Gln-222 in TMD4 tends to lie just at the interface between the polar and non-polar faces of the transmembrane domain (Fig. 7). Furthermore, Thr-114 and Gln-222 are right in the center of the helices, where as Asn-124 and Gln-526 are much deeper, toward the cytoplasmic end of the transmembrane domains (Fig. 7). Considering the strong affect of these mutants on the kinetic parameters coupled to their positioning in the amphiphatic face of the helices, it appears likely that these domains line the translocation channel of the transporter. Among the remaining transmembrane domains targeted in this study, one of the residues targeted in TMD2, TMD6, and TMD7 showed a moderate defect, whereas a second residue in this domain showed a mild or negligible loss in functional activity. These domains might, thus, be peripherally or indirectly involved in the transport process. In contrast, although we targeted two residues in TMD3 and three residues in TMD10 mutation to alanine, none of these mutations

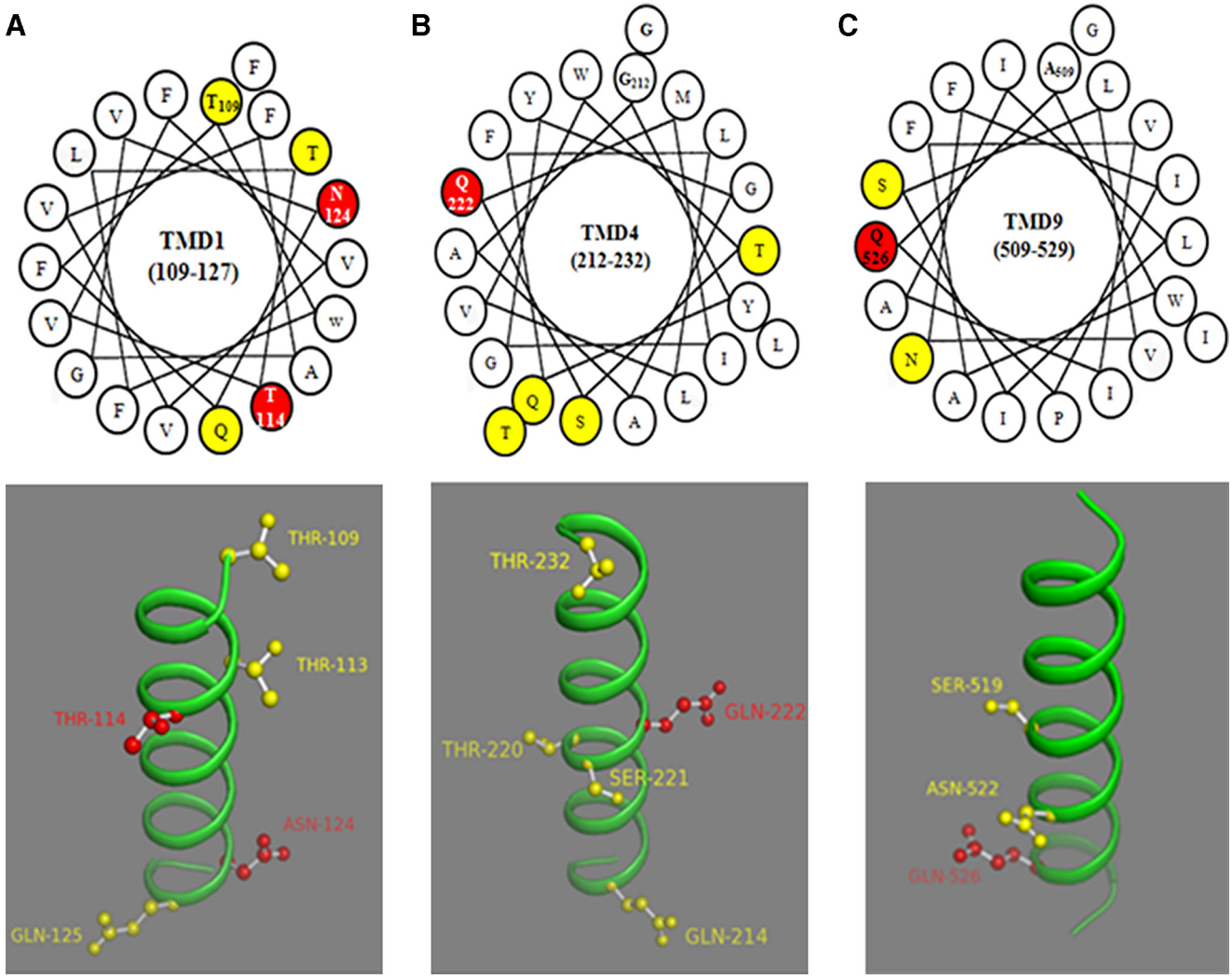

FIGURE 7. **Residues Thr-114 and Asn-124 in TMD1, Gln-222 in TMD4, and Gln-526 in TMD9 critical for the transport activity of Hgt1p fall on the hydrophilic face of the respective transmembrane domains.** The *upper panel* presents the helix wheel projection, and the *lower panel* presents the side view of the helix (shown in *green*), with the extracellular side kept on the *top*. The key residues subjected to alanine mutagenesis in this study are colored *red*, whereas all the other polar residues in the TMDs are colored *yellow*. The side view of the TMDs was drawn using the PyMol Molecular viewer (Version 0.99). *A*, TMD1. *B*, TMD4. *C*, TMD9.

showed a significant effect on activity, leaving these domains open for further exploration for their role in forming the translocation channel.

Among the two intracellular regions 537–568 and 707–724 selected for mutational analysis in this study, only the domain stretching the region 537–568 was found to be crucial for the transporter activity. These two regions, although weakly predicted as putative transmembrane domains, have not been considered as TMDs in the final model because of their proline-rich nature (33). However, three of the charged residues, Lys-562, Glu-544, and Arg-554, belonging to the highly conserved proline rich motif, ^{544}E*X*I*X*GYX_2PG(R/K)P*X*AX_4KX_2G^{565}, in this region were found to be critical for the translocation activity of the protein (Table 3). Previously, experimental characterization of the conserved proline residues in the transmembrane domains of the voltage-gated potassium (K_v) channels and ligand gated channels has revealed that these proline residues provide a hinge or kink that is proposed to act as a molecular switch to link the conformational changes in the protein with the substrate translocation (38). Similarly, the conserved prolines in the vicinity of the catalytic cysteines as PCX_{2-3}P motif in the transmembrane domain of DsbD, an integral membrane oxidoreductase in *E. coli*, have been shown to be critical for the functionally important conformational flexibility of the protein (39). The results of the mutational analysis in our study and the high degree of conservation of the region 537–568 in Hgt1p (Fig. 6 and data not shown) seem to point toward an important role of this proline-rich region in protein activity, and indeed, we have recently observed that Pro-555 is important for transport activity of Hgt1p.[4] It is likely that the presence of the conserved proline residues in the region might confer a high degree of conformational flexibility to this region needed for substrate translocation or enable the domain to partially transverse the membrane, forming an inverted loop that could be critical for substrate binding or translocation.

[4] C. V. Srikanth and A. K. Bachhawat, unpublished data.

Of particular interest were the two glutamine residues, Gln-222 in TMD4 and Gln-526 in TMD9. Although replacement of the former with alanine resulted in a nearly 4-fold increase in K_m value and almost a complete loss in the catalytic turnover of the transporter, Q526A mutant showed a nearly 8-fold decrease in the K_m values without a significant effect on V_{max}. Furthermore, Gln-222 was found conserved among different OPT members, whereas Gln-526 was present only in Pgt1 but not in the other functionally characterized oligopeptide transporters. This differential pattern of conservation and effect of mutations of Gln-222 and Gln-526 becomes particularly remarkable as Pgt1, like Hgt1p, is the only other PT member characterized to transport glutathione with high affinity, whereas all the other three PT members, AtOpt4, CaOpt1, and Isp4, have been shown to transport tetrapeptides and pentapeptides but do not transport glutathione (4, 7, 35, 36). Taken together, the results suggest that although both glutamine residues participate in substrate transport, Gln-526 is critical in identifying glutathione as substrate, whereas Gln-222 recognizes a structural feature common to oligopeptides, including glutathione, a modified tripeptide. In further considering the dramatic effect of mutation on Gln-222 on K_m and V_{max}, it could be that the residue might not be directly involved in substrate binding but might be needed for the translocation of substrate and, hence, its influence on substrate binding as well. In contrast Gln-526 appears to be strictly important for glutathione binding/recognition.

Considering the role of Gln-526 as a key residue in identification of glutathione as a substrate, it might be interesting to probe the role of the other polar residues with limited conservation only among the glutathione transporters (Fig. 6). Such residues with limited conservation across the family have been shown to be critical determinants of substrate selectivity among the other transporters. For instance, among 18 homologues of the sugar transporting family in *S. cerevisiae*, only the high affinity galactose transporter (Gal2p) contains tyrosine as a central aromatic acid in TMD10, whereas all the other 17 homologues, including Hxt2p, a high affinity glucose transporter, contain phenylalanine at the corresponding site. Experimental studies have shown that the presence of tyrosine in Gal2p is crucial for differential recognition of galactose and glucose between the two transporters (40, 41). Similarly, a single difference of a glycine residue in TMD6 of GLYT1 for a serine residue at the corresponding position in GLYT2 is sufficient to explain the ability of GLYT1 to transport glycine and its *N*-methyl derivative, sarcosine, whereas GLYT2 transports only glycine (16).

Although Hgt1p and the *S. pombe* orthologue of the same family, Pgt1, are the only two high affinity glutathione transporters known (K_m in the range of 45–65 μM), low affinity transporters of glutathione have been described and include the MRP family of transporters (MRPs in mammals, Ycf1p in yeast) that transport glutathione with low affinity (K_m in the range of 10 mM) and glutathione conjugates but belong to a very distinct family, the ABC transporter superfamily (42). Interestingly, mutational analysis of charged residues in MRP1 led to the identification of key lysine residues that upon replacement with either Asp or Leu results in selective loss of transport of glutathione or its conjugate cysteinyl leukotriene 4 (LTC4), with no discernible effect on the transport of other organic acids or methotrexate drug (17). This is particularly interesting when one considers that even more direct evidence for a role of glutamine and lysine residues in glutathione binding has also been obtained from the crystal structure of a *S. cerevisiae* glutaredoxin (Grx1) bound to glutathione (43), where it was observed that a conserved glutamine and lysine residue are involved in anchoring the glycine moiety of the substrate by a hydrogen-bonding network. A similar role for a glutamine residue has been identified in other glutaredoxins and glutathione *S*-transferases (44–46).

In conclusion, the findings described in this report have enabled us to generate the first structural insights into the functioning of a high affinity glutathione transporter, Hgt1p, laying a platform for a more detailed investigation into the importance of these residues and the TMDs 1, 4, and 9 in the transporter activity of Hgt1p. Considering that members of the OPT family have been implicated in metal and oligopeptide distribution and development processes in plants and mating and survival under adverse conditions in fungi, the insights gained with Hgt1p could pave the way for future efforts to understand and even manipulate the other OPT members.

Acknowledgments—Assistance provided by Wahengbam Romi in construction of some of the alanine mutants and by Anil Thakur in construction of K562R/L mutants and performance of confocal studies with these mutants is acknowledged. We thank Dr. Alok Mondal and Deepak Bhatt for help in acquiring confocal images. We also thank Manish Datt for drawing the side view of TMDs using the PyMol Viewer.

REFERENCES

1. Bourbouloux, A., Shahi, P., Chakladar, A., Delrot, S., and Bachhawat, A. K. (2000) *J. Biol. Chem.* **275,** 13259–13265
2. Yen, M. R., Tseng, Y. H., and Saier, M. H., Jr. (2001) *Microbiology* **147,** 2881–2883
3. Lubkowitz, M. (2006) *Genet. Eng.* **27,** 35–55
4. Thakur, A., Kaur, J., and Bachhawat, A. K. (2008) *FEMS Yeast Res.* **8,** 916–929
5. Stacey, M. G., Patel, A., McClain, W. E., Mathieu, M., Remley, M., Rogers, E. E., Gassmann, W., Blevins, D. G., and Stacey, G. (2008) *Plant Physiol.* **146,** 589–601
6. Waters, B. M., Chu, H. H., Didonato, R. J., Roberts, L. A., Eisley, R. B., Lahner, B., Salt, D. E., and Walker, E. L. (2006) *Plant Physiol.* **141,** 1446–1458
7. Osawa, H., Stacey, G., and Gassmann, W. (2006) *Biochem. J.* **393,** 267–275
8. Hauser, M., Donhardt, A. M., Barnes, D., Naider, F., and Becker, J. M. (2000) *J. Biol. Chem.* **275,** 3037–3041
9. Kaur, J., Srikanth, C. V., and Bachhawat, A. K. (2009) *FEMS Yeast Res.*, in press
10. Falcón-Pérez, J. M., Martínez-Burgos, M., Molano, J., Mazón, M. J., and Eraso, P. (2001) *J. Bacteriol.* **183,** 4761–4770
11. Falcón-Pérez, J. M., Mazón, M. J., Molano, J., and Eraso, P. (1999) *J. Biol. Chem.* **274,** 23584–23590
12. Fann, M., Davies, A. H., Varadhachary, A., Kuroda, T., Sevier, C., Tsuchiya, T., and Maloney, P. C. (1998) *J. Membr. Biol.* **164,** 187–195
13. Arastu-Kapur, S., Arendt, C. S., Purnat, T., Carter, N. S., and Ullman, B. (2005) *J. Biol. Chem.* **280,** 2213–2219
14. Arastu-Kapur, S., Ford, E., Ullman, B., and Carter, N. S. (2003) *J. Biol. Chem.* **278,** 33327–33333
15. Valdés, R., Liu, W., Ullman, B., and Landfear, S. M. (2006) *J. Biol. Chem.*

281, 22647–22655
16. Vandenberg, R. J., Shaddick, K., and Ju, P. (2007) *J. Biol. Chem.* **282,** 14447–14453
17. Haimeur, A., Conseil, G., Deeley, R. G., and Cole, S. P. (2004) *Mol. Pharmacol.* **65,** 1375–1385
18. Hauser, M., Kauffman, S., Naider, F., and Becker, J. M. (2005) *Mol. Membr. Biol.* **22,** 215–227
19. Oldham, M. L., Khare, D., Quiocho, F. A., Davidson, A. L., and Chen, J. (2007) *Nature* **450,** 515–521
20. Abramson, J., Smirnova, I., Kasho, V., Verner, G., Kaback, H. R., and Iwata, S. (2003) *Science* **301,** 610–615
21. Lemieux, M. J., Song, J., Kim, M. J., Huang, Y., Villa, A., Auer, M., Li, X. D., and Wang, D. N. (2003) *Protein Sci.* **12,** 2748–2756
22. Yamashita, A., Singh, S. K., Kawate, T., Jin, Y., and Gouaux, E. (2005) *Nature* **437,** 215–223
23. Sambrook, J., Fritsch, E. F., and Maniatis, T. (1989) *Molecular Cloning: A Laboratory Manual*, Cold Spring Harbor Press, Cold Spring Harbor, New York
24. Guthrie, C., Fink, G. R., Simon, M. I., and Abelson, J. N. (1991) *Methods Enzymol.* **194,** 3–37
25. Kaur, J., and Bachhawat, A. K. (2009) *Anal. Biochem.* **384,** 348–349
26. Severance, S., Chakraborty, S., and Kosman, D. J. (2004) *Biochem. J.* **380,** 487–496
27. Thompson, J. D., Gibson, T. J., Plewniak, F., Jeanmougin, F., and Higgins, D. G. (1997) *Nucleic Acids Res.* **25,** 4876–4882
28. Tusnády, G. E., and Simon, I. (2001) *Bioinformatics* **17,** 849–850
29. Krogh, A., Larsson, B., von Heijne, G., and Sonnhammer, E. L. (2001) *J. Mol. Biol.* **305,** 567–580
30. Jones, D. T., Taylor, W. R., and Thornton, J. M. (1994) *Biochemistry* **33,** 3038–3049
31. Rost, B., Fariselli, P., and Casadio, R. (1996) *Protein Sci.* **5,** 1704–1718
32. Claros, M. G., and von Heijne, G. (1994) *Comput. Appl. Biosci.* **10,** 685–686
33. Wiles, A. M., Naider, F., and Becker, J. M. (2006) *Res. Microbiol.* **157,** 395–406
34. Srikanth, C. V., Vats, P., Bourbouloux, A., Delrot, S., and Bachhawat, A. K. (2005) *Curr. Genet.* **47,** 345–358
35. Lubkowitz, M. A., Barnes, D., Breslav, M., Burchfield, A., Naider, F., and Becker, J. M. (1998) *Mol. Microbiol.* **28,** 729–741
36. Lubkowitz, M. A., Hauser, L., Breslav, M., Naider, F., and Becker, J. M. (1997) *Microbiology* **143,** 387–396
37. Miyake, T., Kanayama, M., Sammoto, H., and Ono, B. (2002) *Mol. Genet. Genomics* **266,** 1004–1011
38. Sansom, M. S., and Weinstein, H. (2000) *Trends Pharmacol. Sci.* **21,** 445–451
39. Hiniker, A., Vertommen, D., Bardwell, J. C., and Collet, J. F. (2006) *J. Bacteriol.* **188,** 7317–7320
40. Kasahara, M., and Maeda, M. (1998) *J. Biol. Chem.* **273,** 29106–29112
41. Kasahara, M., Shimoda, E., and Maeda, M. (1997) *J. Biol. Chem.* **272,** 16721–16724
42. Ballatori, N., Hammond, C. L., Cunningham, J. B., Krance, S. M., and Marchan, R. (2005) *Toxicol. Appl. Pharmacol.* **204,** 238–255
43. Yu, J., Zhang, N. N., Yin, P. D., Cui, P. X., and Zhou, C. Z. (2008) *Proteins* **72,** 1077–1083
44. Dirr, H., Reinemer, P., and Huber, R. (1994) *Eur. J. Biochem.* **220,** 645–661
45. Oakley, A. J., Lo Bello, M., Battistoni, A., Ricci, G., Rossjohn, J., Villar, H. O., and Parker, M. W. (1997) *J. Mol. Biol.* **274,** 84–100
46. Johansson, C., Kavanagh, K. L., Gileadi, O., and Oppermann, U. (2007) *J. Biol. Chem.* **282,** 3077–3082